Estuarine, Coastal and Shelf Science 284 (2023) 108271

Contents lists available at ScienceDirect

Estuarine, Coastal and Shelf Science

journal homepage: www.elsevier.com/locate/ecss

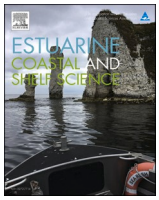

Influence of glacier type on bloom phenology in two Southwest Greenland fjords

A.E. Stuart-Lee [a,*], J. Mortensen [b], T. Juul-Pedersen [b], J.J. Middelburg [c], K. Soetaert [a], M.J. Hopwood [d], A. Engel [e], L. Meire [a,b]

[a] Department of Estuarine and Delta Systems, Royal Netherlands Institute for Sea Research, Yerseke, the Netherlands
[b] Greenland Climate Research Centre, Greenland Institute of Natural Resources, Nuuk, Greenland
[c] Department of Earth Sciences, Geosciences, Utrecht University, Utrecht, the Netherlands
[d] Department of Ocean Science and Engineering, Southern University of Science and Technology, Shenzhen, China
[e] Marine Biogeochemistry, GEOMAR Helmholtz Centre for Ocean Research Kiel, Kiel, Germany

A B S T R A C T

Along Greenland's coastline, the magnitude and timing of primary production in fjords is influenced by meltwater release from marine-terminating glaciers. How local ecosystems will adapt as these glaciers retreat onto land, forcing fundamental changes in hydrography, remains an open question. To further our understanding of this transition, we examine how marine- and land-terminating glaciers respectively influence fjord bloom phenology. Between spring and autumn 2019, we conducted along-fjord transects of hydrographic variables, biogeochemical properties and pico- and nanophytoplankton counts to illustrate the contrasting seasonal bloom dynamics in the fjords Nuup Kangerlua and Ameralik. These fjords are in the same climatic region of west Greenland but influenced by different glacial structures. Nuup Kangerlua, a predominantly marine-terminating system, was differentiated by its sustained second summer bloom and high Chl *a* fluorescence in summer and autumn. In Ameralik, influenced by a land-terminating glacier, we found higher abundances of pico- and nanophytoplankton, and high cyanobacteria growth in autumn. The summer bloom in Nuup Kangerlua is known to be coincident with subglacial freshwater discharge sustaining renewed nutrient supply to the fjord. We observe here that the intermediate baroclinic circulation, which creates an inflow at subsurface depths, also plays an important role in increasing nutrient availability at shallower depths and potentially explains the distribution of primary producers. Our observations suggest that the retreat of marine-terminating glaciers onto land, with consequent increases in surface water temperature and stratification, and reduced light availability, may alter the magnitude, composition, and distribution of summer productivity.

1. Introduction

The Greenland Ice Sheet is melting at a greater rate than it has for at least the last 350 years (Trusel et al., 2018). Along the coast of Greenland, this translates to an increasing quantity of freshwater runoff entering the surrounding fjords and rapid retreat of the glaciers at the ocean interface (King et al., 2020; Mankoff et al., 2020). Based on a 46-year mass balance reconstruction of the Greenland Ice Sheet, the more than 200 glaciers that are marine-terminating are estimated to be responsible for approximately two thirds of the ice sheet mass loss in recent decades (Howat and Eddy, 2011; Mouginot et al., 2019).

(Sub-)Arctic fjords influenced by marine-terminating (tidewater) glaciers are observed to support productive marine ecosystems, closely bound to their unique hydrodynamics. Subglacial discharge plumes cause upwelling of nutrient-rich seawater, indirectly fertilising the surface waters. This has been observed to stimulate primary production during the meltwater season in tidewater glacier fjords across the Arctic (Calleja et al., 2017; Meire et al., 2017; Kanna et al., 2018; Cape et al., 2019; Halbach et al., 2019; Bhatia et al., 2021). Other mechanisms associated with glacial runoff from both land- and marine-terminating glaciers may also contribute to this effect. Increased nutrient availability in the photic zone is one such factor, and it occurs through the enhancement of the estuarine circulation characteristic of glacial fjords (Rysgaard et al., 2003; Dunse et al., 2022). Close to glacier termini, however, the delivery of glacial particles limits light availability for phytoplankton, restricting the potential for production in these systems (Murray et al., 2015). This counter-effect has been well documented in Kongsfjorden, Svalbard, through along-fjord gradients of phytoplankton productivity and abundance (Halbach et al., 2019; Szeligowska et al., 2021). The observed spatial gradients in Kongsfjorden also translate to the composition of both primary and secondary producers (Piwosz et al., 2009; Halbach et al., 2019; Trudnowska et al., 2020). Lower diversity in

* Corresponding author.
E-mail addresses: alice.stuart-lee@nioz.nl (A.E. Stuart-Lee), jomo@natur.gl (J. Mortensen), thpe@natur.gl (T. Juul-Pedersen), j.b.m.middelburg@uu.nl (J.J. Middelburg), karline.soetaert@nioz.nl (K. Soetaert), mark@sustech.edu.cn (M.J. Hopwood), aengel@geomar.de (A. Engel), lorenz.meire@nioz.nl (L. Meire).

https://doi.org/10.1016/j.ecss.2023.108271
Received 21 September 2022; Received in revised form 7 December 2022; Accepted 17 February 2023
Available online 26 February 2023

phytoplankton species at the glacier fronts than in the central and outer fjord regions has been observed in summer, with increasing contributions of dinoflagellates and diatoms to the community with distance from the glaciers (Halbach et al., 2019).

Across Greenland, the largest increases in freshwater runoff in recent decades have been recorded in the west (Mernild and Liston, 2012). A well-studied fjord in this region is Nuup Kangerlua (Godthåbsfjord), where seasonal productivity is characterised by annual blooms occurring in spring and summer/autumn (Juul-Pedersen et al., 2015; Krawczyk et al., 2015). These productive blooms have been partially attributed to the influence of marine-terminating glaciers. This is due to both the upwelling effect of subglacial discharge as well as the high silicate:nitrate ratio of glacial meltwater that stimulates diatom growth, an important component of both spring and summer/autumn blooms (Juul-Pedersen et al., 2015; Krawczyk et al., 2015; Meire et al., 2016, 2017).

Few land-terminating glacier fjords have been subject to multi-season investigation, with Young Sound in northeast Greenland being a notable exception. Seasonal bloom development in Young Sound has been contrasted with that of Nuup Kangerlua. Key differences have been attributed to different modes of freshwater supply (land-vs marine-terminating glaciers), leading to divergences in patterns of summertime primary production (Meire et al., 2017). While the shorter open-water period and higher latitude location are key reasons for low annual productivity in Young Sound, this is also compounded by the increased stratification and reduced light availability resulting from high particle load carried by meltwater from land-terminating glaciers (Meire et al., 2017; Holding et al., 2019; Randelhoff et al., 2020). Glacial influence has also been associated with a gradient in phytoplankton cell size. Small cells (<10 μm) have been observed dominating close to the source of runoff where the surface water is turbid and brackish, followed by an increase in cell size towards the fjord mouth (Middelbo et al., 2017).

Conclusively disentangling the underlying processes and mechanisms that explain these inter-fjord differences remains challenging because of the few detailed field surveys available. Attempts to scale to a pan-Greenlandic perspective are limited by the scarcity of well-studied field sites and the vastly heterogeneous nature of fjords (Straneo et al., 2019). There is a general bias in the oceanographic literature towards studies of a few large systems (e.g., Bowdoin, Jacobshaven Isbare, Nioghalvfjerdsbræ, Nuup Kangerlua, Sermilik) that account for a disproportionately large fraction of annual liquid and solid freshwater discharge but are not representative of the hundreds of small glacier fjords (such as Young Sound) that surround Greenland (Straneo et al., 2019).

In the context of climate change, it is important to understand how marine ecosystems will respond to the combined effects of glacier retreat and increasing freshwater discharge, what feedbacks this will induce on marine producers and the carbon cycle, and how this will affect other ecosystem services such as fisheries. Whilst the physical and chemical dynamics of multiple glacier fjord systems in Greenland have been explored, and primary production data are available for a few systems, ecosystem dynamics are less well described with moderately extensive work only available at Nuup Kangerlua and Young Sound (e.g. Arendt et al., 2010; Bridier et al., 2021). In this study we present a seasonal comparison of biogeochemical properties (nutrients and suspended particulate matter), pico- and nanophytoplankton cell counts and bloom dynamics in Nuup Kangerlua and Ameralik, the neighbouring fjord to the south which is influenced by a land-terminating glacier (Fig. 1). We compare these two fjords from the same climate-vulnerable region of

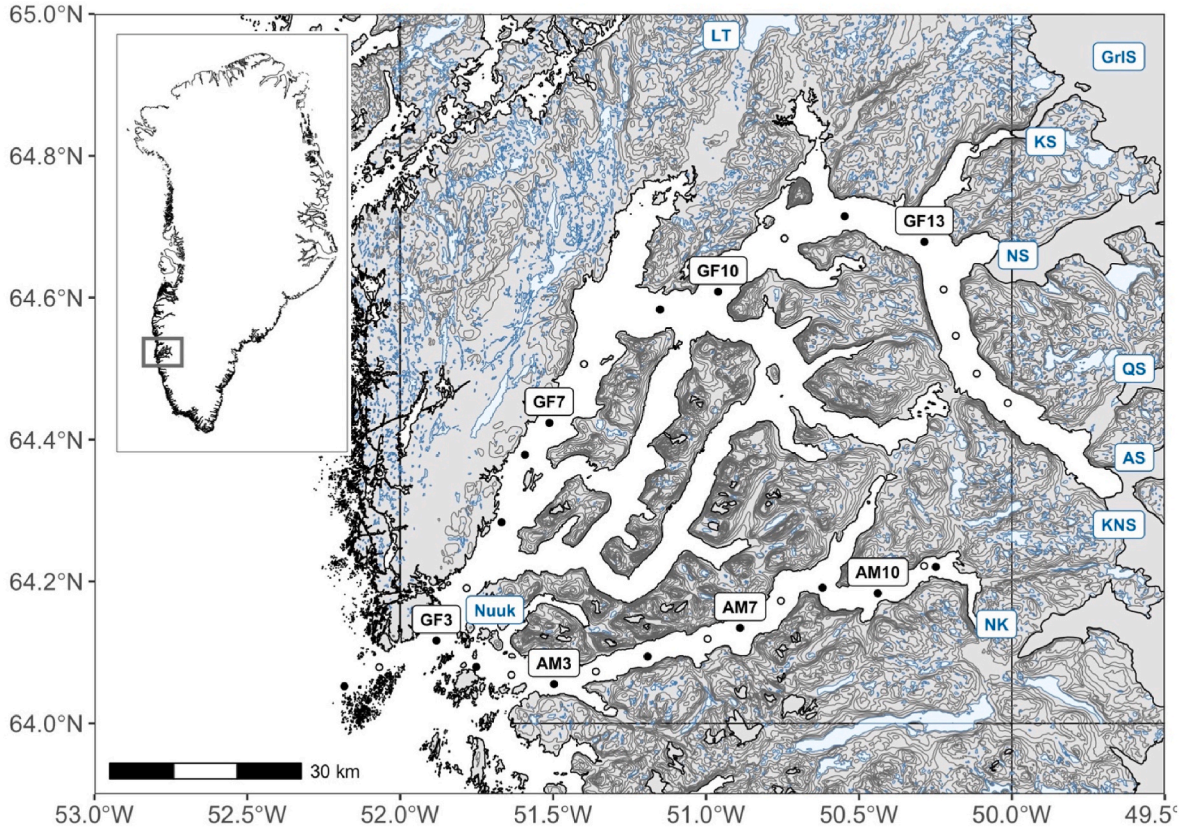

Fig. 1. Study site. Positions of the sampling stations (circles) in Nuup Kangerlua (GF) and Ameralik (AM). Key stations are annotated GF_x for Nuup Kangerlua and AM_x for Ameralik, as per prior work. Acronyms represent the Greenland Ice Sheet (GrIS), marine-terminating glaciers (Akullersuup Sermia, AS, Kangiata Nunaata Sermia, KNS, Narsap Sermia, NS), land-terminating glaciers (Kangilinnguata Sermia, KS, Qamanaarsuup Sermia, QS), and other freshwater sources (Lake Tasersuaq, LT, and Naajat Kuuat, NK) (Adapted from Stuart-Lee et al., 2021.). Solid circles indicate sites at which samples were taken for flow cytometry analysis.

west Greenland, which largely removes factors related to regional differences in climate conditions, the latitude-dependent length of the growth season, and coastal water masses. We hypothesise that large inputs of glacial meltwater from land-terminating glaciers (Ameralik) result in higher abundances of small cells compared to fjords influenced predominantly by marine-terminating glaciers (Nuup Kangerlua). In developing our understanding of the relationship between glaciers and the activity of phytoplankton in connected fjords, we aim to provide insight into how present-day Greenland fjord ecosystems may change with ongoing glacial retreat and increasing freshwater discharge.

2. Materials and methods

2.1. Study site

Nuup Kangerlua (Godthåbsfjord) and Ameralik are neighbouring sill fjords on the west coast of Greenland, close to Nuuk (Fig. 1). Nuup Kangerlua consists of several branches covering an area of ~2013 km^2. Its main branch, where the sampling stations are located, is ~190 km long and the basin reaches a maximum depth of ~620 m. Freshwater and solid ice are delivered to the fjord via three marine-terminating glaciers (Kangiata Nunaata Sermia (KNS), Akullersuup Sermia (AS), and Narsap Sermia (NS), Fig. 1). In terms of annual solid and liquid discharge KNS is the largest; it has a grounding line depth of ~250 m (Mortensen et al., 2013). Glacial rivers deliver freshwater from 3 land-terminating glaciers (Qamanaarsuup Sermia (QS), Kangilinnguata Sermia (KS) and Saqqap Sermersua via Lake Tasersuaq (LT), Fig. 1) into the fjord. Sea ice covers the innermost part of the fjord on a seasonal basis, typically extending from the innermost fjord to station GF13 in winter, and an ice mélange commonly occupies this part of the inner fjord (close to the three marine-terminating glaciers) in summer.

Ameralik shares its mouth region with Nuup Kangerlua, and its entrance is found south of Nuuk. Ameralik is ~75 km long, with an area of ~400 km^2 and a maximum basin depth of ~700 m. Freshwater is delivered from one land-terminating glacier (Kangaasarsuup Sermia) by the glacial river Naajat Kuuat (NK, Fig. 1). No glaciers terminate directly in the fjord, and sea ice is generally not observed except in small quantities near the river in the innermost part of the fjord in winter.

This western region of Greenland experiences strong tides. A tidal range of ~1–5 m is observed in Kobbefjord, a small fjord located between Nuup Kangerlua and Ameralik (Richter et al., 2011). Coastal water masses outside the fjords are described by Rysgaard et al. (2020). In brief, there is an upper layer of relatively cool and fresh southwest Greenland coastal water (CW), and a lower layer of warmer and more saline subpolar mode water (SPMW), further distinguished by an upper layer (uSPMW) and a cooler and less saline deep layer (dSPMW). Occasionally the upper layer of the coastal waters at 64°N is occupied by a cold and relatively saline Baffin Bay Polar Water (BBPW), a winter mode water mass originating in the eastern part of Baffin Bay (Mortensen et al., 2022). Seasonal hydrography and circulation modes have been described extensively for Nuup Kangerlua (Mortensen et al., 2011, 2013, 2014) and for Ameralik in the same year as this study (Stuart-Lee et al., 2021).

2.2. Methods

Along-fjord transects covering 13 stations in Nuup Kangerlua (GF1-GF13) and 12 stations in Ameralik (AM1-AM12; Fig. 1) were sampled in May, July and September 2019 for physical (temperature, salinity, turbidity and PAR), chemical (nutrients, suspended particulate matter) and biological (fluorescence, Chl *a*, phytoplankton) parameters. Favourable ice conditions in September allowed 4 further stations to be sampled in Nuup Kangerlua (GF14-17). Sampling was conducted from the Greenlandic RV Sanna in May, and from the commercial Greenlandic vessels Polar Dive in July and Tulu in September.

At every station, temperature and salinity depth profiles were collected using a SeaBird SBE19plus CTD equipped with additional sensors for fluorescence (Seapoint), turbidity (Seapoint), and PAR (Biospherical QSP- 2350L Scalar). Sensors were calibrated annually by the manufacturer and precision for salinity was typically within the range of 0.005–0.010. Resulting depth profiles from the downward casts were averaged over 1 m vertical depth intervals. Practical salinity scale (PSU) is used throughout the text.

Water sampling was conducted using 5 L Niskin bottles. At every station, water samples for Chl *a* analysis were collected at 1, 5, 10, 15, 20, 30, 40, and 50 m depths. 500 ml was filtered through 25 mm Whatman GF/F filters (0.7 μm pore size, 1 per depth) and frozen at −80 °C (May) or −20 °C (July and September). The filters were extracted in 10 ml 96% ethanol for ~24 h. The Chl *a* concentration was measured with a TD-700 Turner Designs fluorometer before and after the addition of 200 μL 1 M HCl solution and results were calibrated against a Chl *a* standard. Fluorescence measurements from the CTD were calibrated using the Chl *a* concentrations as per Lyngsgaard et al. (2014). In brief, we calculated the ratio of fluorescence to Chl *a* concentration at each sampling depth (using a rolling 3 m mean value of fluorescence), interpolated this ratio across the full depth profile (at 1 m resolution), and used this to estimate the fluorescence.

Water for nutrient analysis (nitrite, nitrate, ammonium, phosphate and silicate) was sampled from 1, 5, 10, 15, 20, 30, 40, 50, 100, and 200 m depth. Two samples for each depth were filtered through 0.45 μm Millipore filters (Q-Max GPF syringe) and stored frozen at −20 °C until analysis using standard colorimetric methods on a Seal QuAAtro autoanalyzer (Grasshoff et al., 1999).

At 16 stations (marked with a solid circle in Fig. 1), water was sampled for flow cytometry analysis. Water was collected at 1, 5, 10, 20, 30, 40, 100, and 200 m, directly from the Niskin bottle into 5 ml cryogenic vials (1 per depth). These were preserved with glutaraldehyde (Sigma-Aldrich) at 1% final concentration, left for ~1 h in a refrigerator at 4 °C and then frozen at −80 °C. Phytoplankton cells were later filtered through a 50 μm net, counted using a flow cytometer (Becton Dickinson FACSCalibur, flow rate 40–42 μL min^{-1}) and grouped by their pigment autofluorescence and forward scattering properties. Pico- and nanophytoplankton communities were partitioned into small, medium and large Chl *a* rich cells and small and large Phycoerythrin rich cells. Phycoerythrin is considered a proxy for *Synechococcus* contributions. Small cells were allocated to picophytoplankton and intermediate and large cells to nanophytoplankton.

At 7 stations (those marked with station labels in Fig. 1) suspended particulate matter was collected by filtering ~2 L water from 1, 10, 20, 30, 40, 100, and 200 m and the deepest sampled depth, onto pre-combusted (4 h at 450 °C) and pre-weighed 25 mm GF/F filters (0.7 μm pore size, 1 per depth). Filtration continued until the filters were clogged (0.75–2 L). For all samples, visible zooplankton were removed with tweezers and filters were then stored at −80 °C (May) or −20 °C (July and September). Samples were analysed as per Grosse et al. (2015). They were decarbonated in a desiccator with fuming hydrochloric acid (37%) and analysed on a Thermo Flash EA1112 elemental analyser coupled to a Thermo Finnigan Delta V isotope ratio mass spectrometer.

All statistical analysis was done using the open-source programming language R (R Core Team, 2013). Tests for correlations between parameters were carried out with the 'stats' package v4.1.0, using the Pearson's product moment correlation coefficient (significance level = 0.05).

3. Results

3.1. Hydrography

Local freshwater runoff is generally low in May (Langen et al., 2015). This is reflected in the highest surface salinities of the studied months and weak stratification in both fjords (Figs. 2 and 3), consistent with

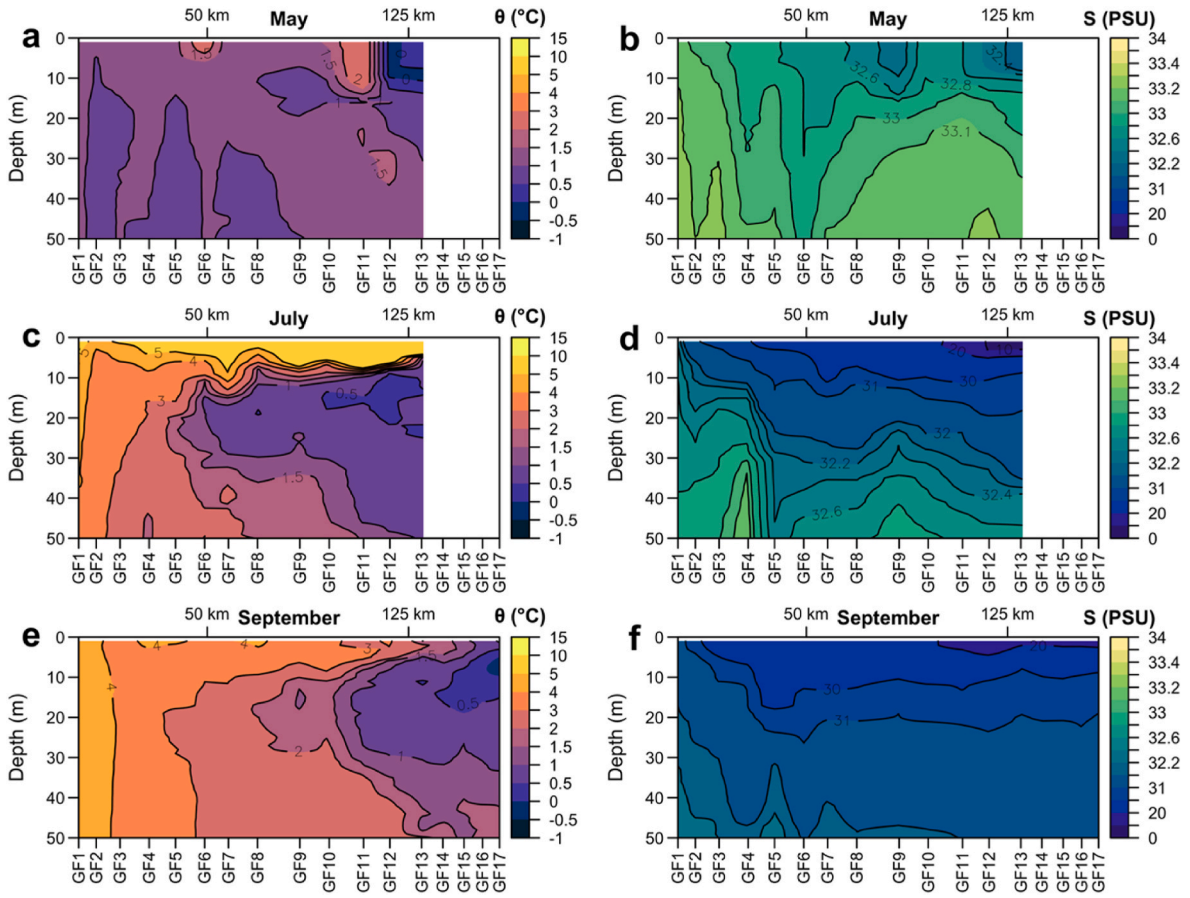

Fig. 2. Nuup Kangerlua upper 50 m potential temperature (a, c, e) and salinity (b, d, f) sections in May, July and September 2019, respectively. Station locations are indicated in Fig. 1. Distances refer to displacement along the transect from the outermost (fjord mouth) station.

prior observations at this time of year (Mortensen et al., 2011, 2013, 2014). The mean T-S properties of the upper 50 m layer were 1.1 °C and 33.0 in Nuup Kangerlua, and 0.5 °C and 33.1 in Ameralik. By July, increased glacial meltwater input (Langen et al., 2015) led to significant surface freshening and accompanying stratification in both fjords, starting in the innermost parts (close to the glacial sources). The upper 50 m layer in Nuup Kangerlua fjord freshened more than that of Ameralik, with a mean salinity of 31.4 compared to 32.1 in Ameralik. While this layer warmed in both fjords as solar insolation increased, this was partially countered in Nuup Kangerlua by the greater influence of meltwater and glacial ice, leaving the upper 50 m layer 1.6 °C cooler than that of Ameralik in July. A stronger thermocline developed in Nuup Kangerlua at 5–10 m depth and the underlying water had low temperatures of 0–1 °C due to subglacial discharge (Fig. 2c). Meanwhile in Ameralik, water in the upper 50 m layer was no cooler than 3 °C (Fig. 3c). Upper water temperatures continued to be higher in Ameralik in the autumn, with the mean temperature of the upper 50 m of Nuup Kangerlua remaining at 2.4 °C, and that of Ameralik rising to 4.9 °C by September. During this transition between July and September the salinity of the upper 50 m layer increased in both fjords, resulting in denser surface waters with some remaining stratification in the inner and central fjords.

3.2. Turbidity, suspended particulate matter and PAR

Throughout the observation period, the inner regions of Nuup Kangerlua and Ameralik were more turbid than the outer regions. This inner-outer fjord gradient was strongest in July when glacial meltwater input was high (Fig. 4a and b, Fig. 5b). At this time of year, turbidity plumes are visible in the surface waters of the inner-Ameralik stations AM10-12 (Fig. 4b) and correspond to the highest recorded concentration of suspended particulate matter (SPM) in this study of 16 mg/L at the innermost sampled station, AM10 (1 m depth, Fig. 5a). This reflects the input of suspended sediment in glacial meltwater from the proglacial river in the inner fjord. Note that, while high, the SPM loads may still underestimate the peak concentration in near-surface waters as the visible particle plume is present in a thin (<1 m) layer. This layer is easily disturbed, for example by boat passage, and is unlikely to be well resolved in CTD data or bottle samples.

North of Nuup Kangerlua, runoff from the land-terminating glacier Saqqap Sermia enters lake Tasersuaq and is then transported into the main fjord branch between stations GF11 and GF12. Surface freshwater runoff originating from Saqqap Sermia is visible in the high turbidity peak (32 FTU) in the upper 10 m layer at station GF12 (Fig. 4a). A plume of elevated turbidity is visible at this location throughout the year in satellite imagery. Further in-fjord, at station GF13, the highest turbidity in July was recorded at ~20 m depth (13 FTU, Fig. 5a), which corresponded to a peak in SPM of 10.5 mg/L and likely relates to the influence of subsurface meltwater discharge from the marine-terminating glacier Narsap Sermia. In the central part of Nuup Kangerlua, at station GF7, there is a subsurface peak in SPM concentration at the same depth (20 m) and similar in magnitude (10.8 mg/L) to that at GF13 (Fig. 5a), but with different properties. The SPM sample from GF7 at 20 m has a lower C:N ratio (7.8 vs 9.7) and more than 10 times the carbon content (1.1 vs 0.1 mg/L) of the SPM sample from GF13 at 20 m. This difference is mirrored in the average properties of the SPM samples from the upper 40 m (Fig. 5c and d). In July there is an in-fjord gradient of increasing SPM concentrations and increasing C:N ratios along both fjords.

In both fjords the increase in SPM during the melt season has an impact on the light conditions, with light generally penetrating to a

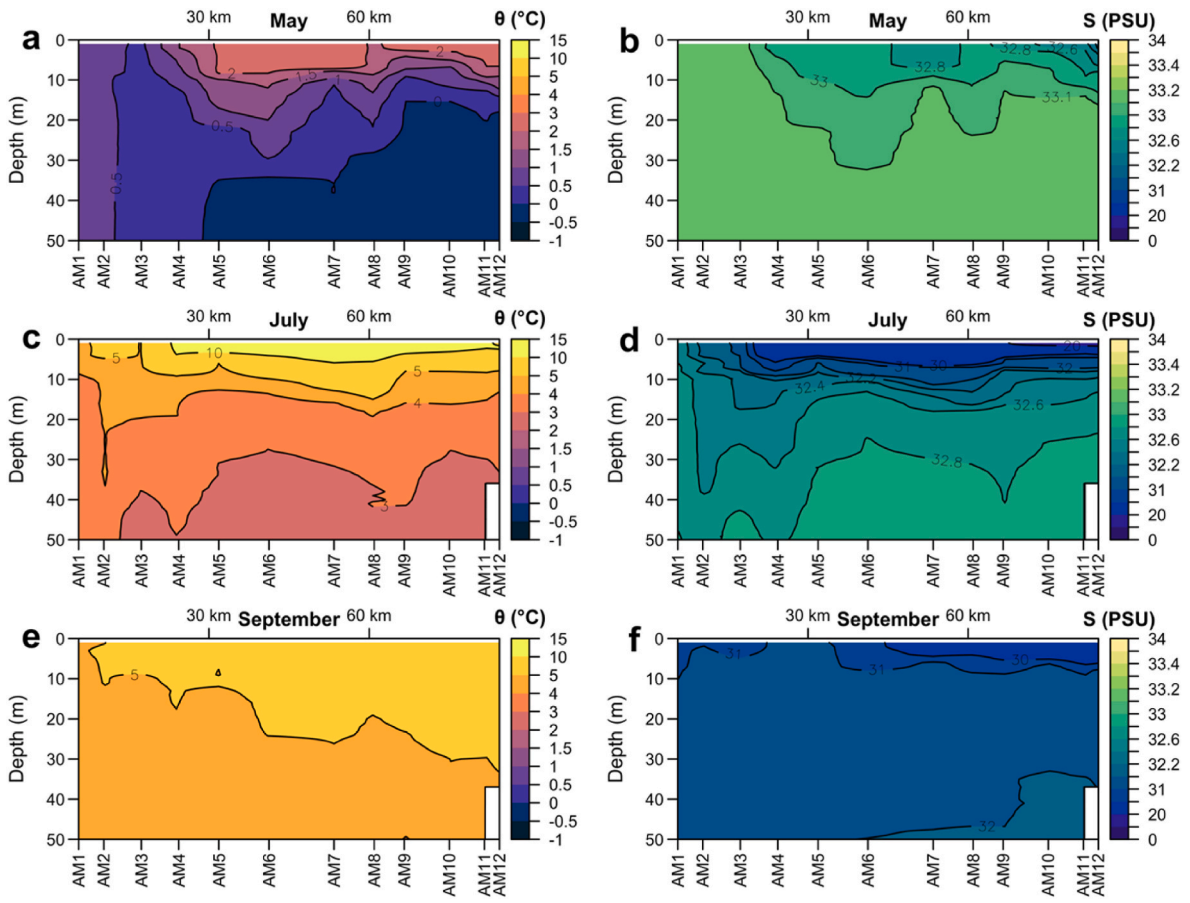

Fig. 3. Ameralik upper 50 m potential temperature (a, c, e) and salinity (b, d, f) sections in May, July and September 2019, respectively. Station locations are indicated in Fig. 1. Distances refer to displacement along the transect from the outermost (fjord mouth) station.

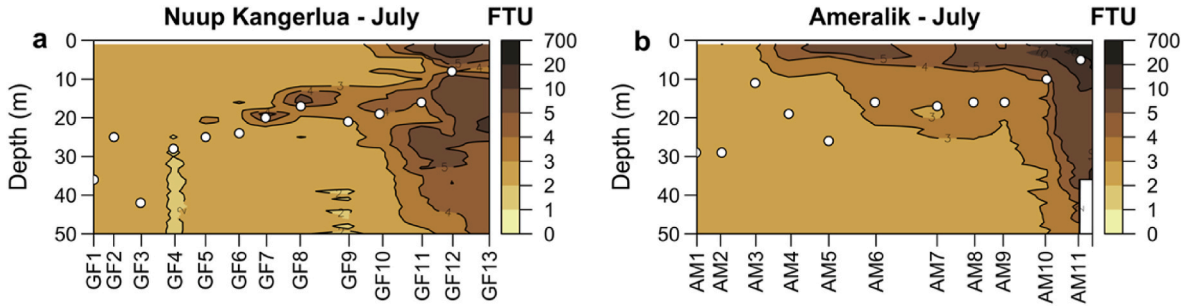

Fig. 4. Turbidity for the upper 50 m in July in (a) Nuup Kangerlua, and (b) Ameralik. White circles indicate the depth at which 1% of surface PAR remains. Station locations are indicated in Fig. 1.

lesser depth at the inner than the outer stations (Fig. 4).

3.3. Nutrients

In both Nuup Kangerlua and Ameralik, we observed along-fjord gradients in nitrate concentrations in May (Fig. 6). In the upper 50 m layer of Nuup Kangerlua, nitrate was lower in the outer fjord than the inner fjord, with mean concentrations ranging from 1.06 μM/L at station GF5 to 5.17 μM/L at the innermost station GF13. The highest nitrate concentration in Nuup Kangerlua in May was 11.3 μM/L, measured at the deepest sampled depth at GF13 of 400 m. In Ameralik, nitrate was more depleted than in Nuup Kangerlua and nutriclines were located deeper in the water column. The fjord gradient was reversed, with higher concentrations in the outer fjord than the inner fjord. Mean upper 50 m nitrate concentrations in May (i.e., mean of the individual data points per cast in Fig. 6) ranged from 0.46 μM/L at station AM12 to 2.64 μM/L at station AM1. Spatial patterns in phosphate concentrations (Fig. S2) generally followed those of nitrate and are largely consistent with prior work in Nuup Kangerlua (e.g., Meire et al., 2017).

By July, surface nutrients were depleted in the upper 20 m of both fjords, with the exception of silicate, which was enriched at the innermost stations due to glacial meltwater runoff (Fig. 6, S1-3). A larger depletion in upper 20 m nitrate occurred in Nuup Kangerlua than in Ameralik. Glacier-related nutrient delivery in Nuup Kangerlua is visible from the subsurface macronutrient peaks at the innermost station GF13. The peaks in nitrate (10.7 μM/L) and phosphate (0.74 μM/L) were at 40 m depth (Fig. 6, S2), and peaks in silicate were at the surface (22.4 μM/L) and at 50 m depth (21.3 μM/L, Fig. S1). At station AM10, there was a

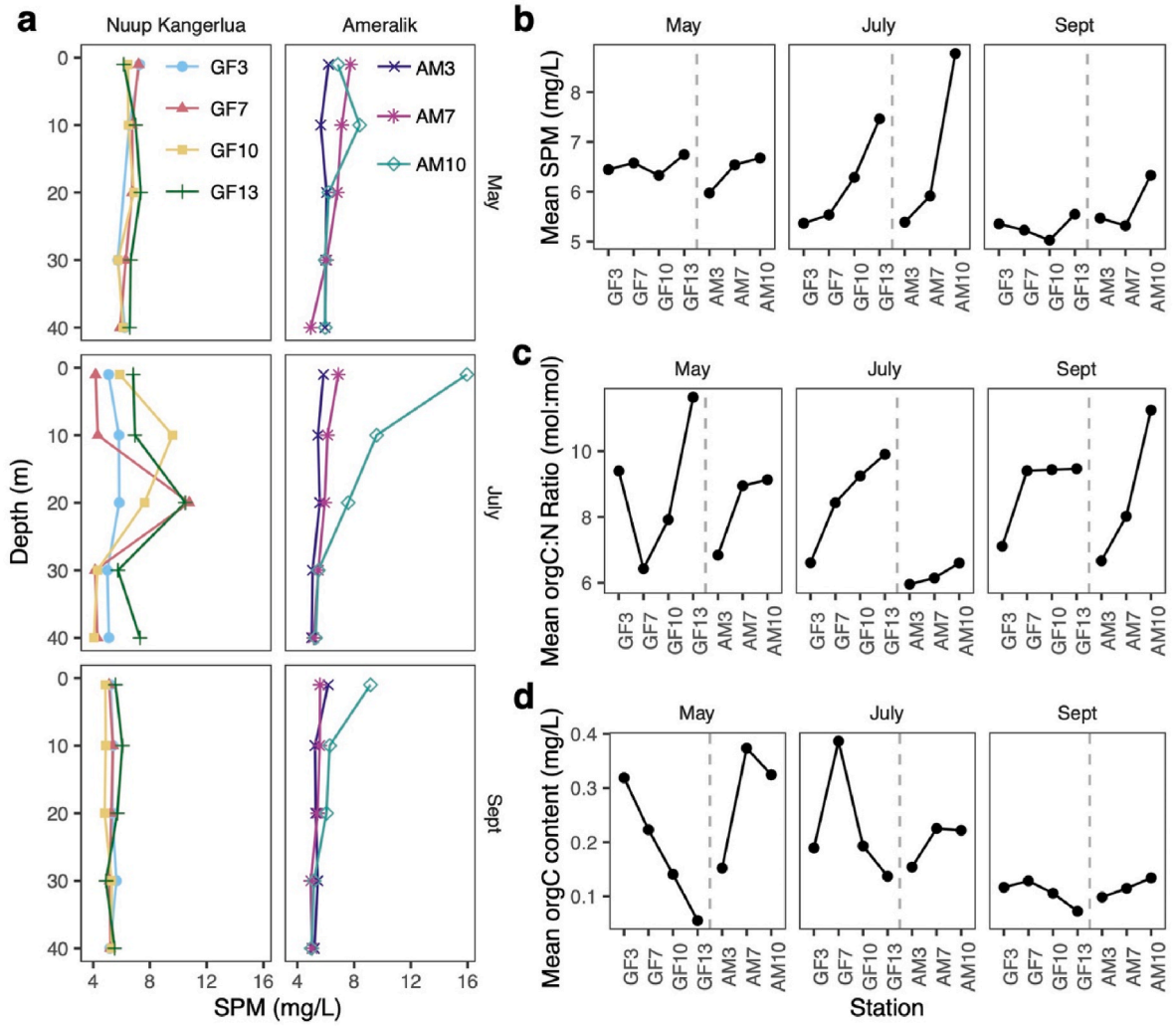

Fig. 5. (a) Upper 40 m depth profiles of suspended particulate matter (SPM, mg/L). (b) Mean SPM concentration (mg/L), (c) mean OrgC:N ratio (mol:mol), and (d) mean organic carbon content (mg/L) of SPM samples from the upper 40 m layer.

silicate peak of 15.9 μM/L at the surface, but no clear enrichment in nitrate or phosphate (Figs. S1–2). This is consistent with the expected concentrations of macronutrients in runoff in the region (Meire et al., 2016).

Ammonium increased in the upper 50 m layer of both fjords through the sampled period (May to September). The highest mean concentrations in the upper 50 m layer were 1.0 μM/L for Nuup Kangerlua and 1.3 μM/L for Ameralik, both measured in September.

Low nutrient concentrations in glacial meltwater are indicated by positive relationships between nitrate/phosphate and salinity throughout the study period. Conversely, silicate showed a negative relationship due to its higher concentration in glacial meltwater, as previously reported by Meire et al. (2016).

3.4. *Fluorescence and pico- and nanophytoplankton*

In May 2019, the highest Chl *a* concentrations in both fjords were found in the upper 10 m layer (Fig. 7a and b). Chl *a* concentrations were higher in Ameralik than in Nuup Kangerlua at this time, with a mean upper 40 m concentration of 4.6 μg/L in Ameralik (stations AM1 - AM12) compared to 2.9 μg/L in Nuup Kangerlua (stations GF1 - GF13, Fig. 8a). In Nuup Kangerlua, small phytoplankton abundances were higher in the outer fjord than the inner fjord, with the highest picophytoplankton (<2 μm) abundance of 18900 cells/ml found at station GF3 (10 m) and the highest nanophytoplankton (2–20 μm) abundance of 3100 cells/ml at station GF7 (1 m). This gradient was reversed for Ameralik, with the highest pico- and nanophytoplankton abundances recorded at station AM12 (13100 and 6420 cells/ml respectively, both at 5 m).

Between May and July, Chl *a* concentrations in the upper 40 m declined throughout Ameralik but increased at the inner fjord stations of Nuup Kangerlua (GF9 - GF13, Fig. 8a). Picophytoplankton abundance in July in Nuup Kangerlua was at its lowest level of the observation period (May to September), while nanophytoplankton abundance had increased (Fig. 8b and c). In contrast, there was a large increase in picophytoplankton in Ameralik, with the mean upper 40 m picophytoplankton count increasing from 5250 cells/ml in May to 15800 cells/ml in July. The highest concentrations remained in the upper 10 m layer but shifted in-fjord to station AM9.

By September, Chl *a* in the upper 40 m layer was relatively low in both fjords (Fig. 8a), though some areas of high Chl *a* biomass remained in the central and inner parts of Nuup Kangerlua at ~10 m depth between stations GF9 and GF17 (Fig. 7e). In Nuup Kangerlua, picophytoplankton abundances increased up to a maximum of 11300 cells/ml (station GF6, 1 m) while nanophytoplankton numbers were comparable to those in July. A larger increase in picophytoplankton cell counts was observed in Ameralik in September. The mean upper 40 m concentration of 46700 cells/ml was more than double the July figure (Fig. 8b). The highest picophytoplankton abundances were measured in the upper 10 m layer and the maximum was 195000 cells/ml (station AM10, 5 m).

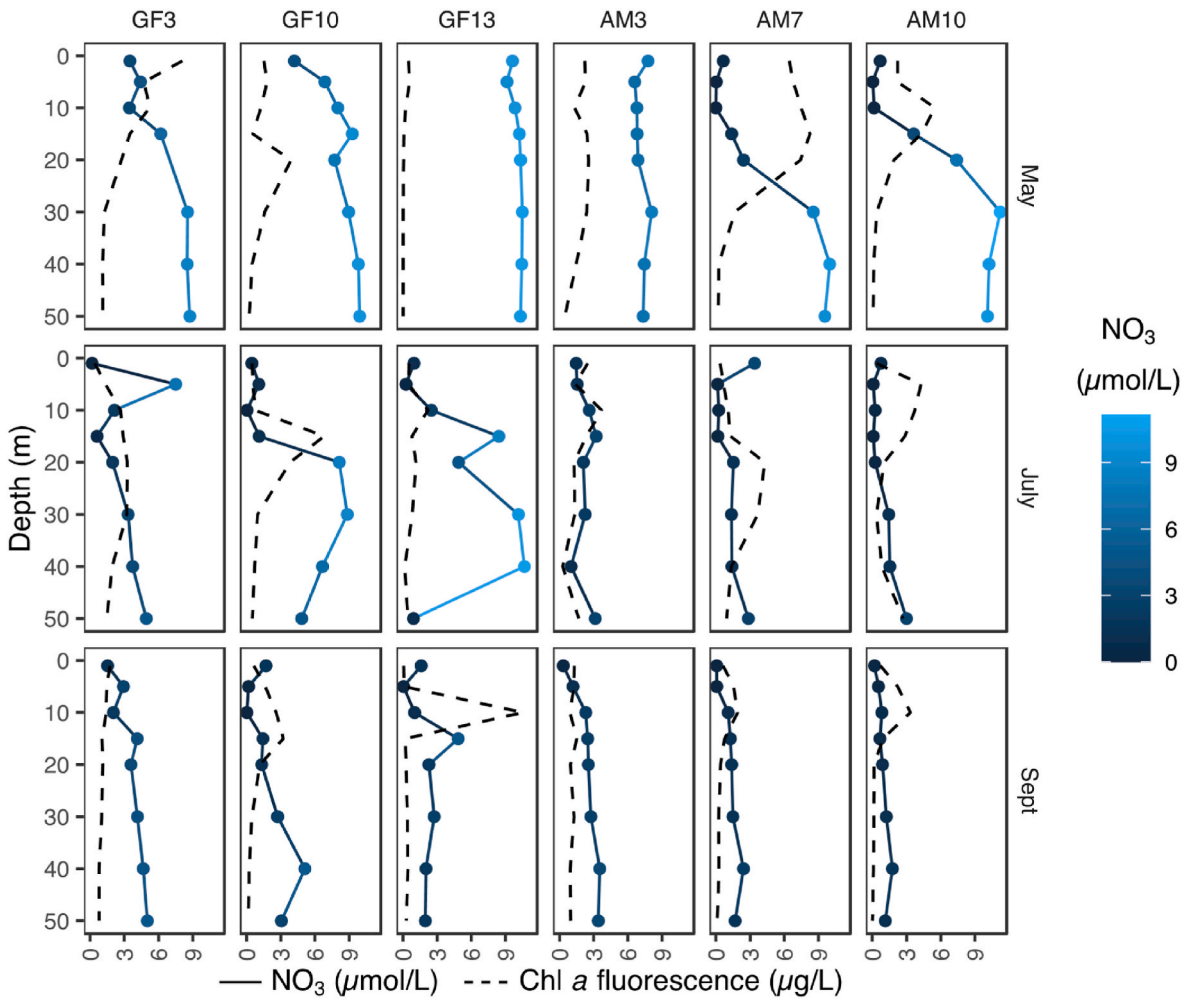

Fig. 6. Upper 50 m depth profiles of nitrate concentrations (solid line with points) and Chl *a* fluorescence (dashed line) at selected stations in May, July and September 2019. Lighter shading highlights higher concentrations.

This fjord-wide increase in Ameralik was driven by *Synechococcus* growth, largely occurring at ~10 m depth in the central and inner parts of the fjord. At this time, there was a strong positive correlation ($r = 0.87$, $p < 0.005$) between the *Synechococcus* cell counts and the nitrogen concentration in SPM.

4. Discussion

4.1. Seasonal bloom dynamics

4.1.1. May

In May, both fjords were characterised by low surface nutrient concentrations and corresponding maxima in Chl *a* (Figs. 6 and 7a,b), though the respective bloom phases were not aligned. Compared to Nuup Kangerlua, the upper waters of Ameralik were lower in nutrients, had deeper nutriclines, and higher Chl *a*, suggesting that Ameralik was in a more developed phase of the spring bloom than Nuup Kangerlua.

Blooms in these systems are initially triggered by increasing insolation alongside high nutrient concentrations. They are facilitated further by the development of a weak surface stratification from heat exchange and surface runoff (which likely consists mainly of snow melt). Weak surface stratification is a potential barrier to nutrient availability when nutrient concentrations are depleted (Randelhoff et al., 2020), but it also provides the advantage of keeping the phytoplankton in the euphotic zone (e.g., Tremblay et al., 2006, 2008). When nutrients are not limiting production at the start of the bloom, the mixed layer depth can in this way influence its timing, with a shallower mixed layer initiating an earlier bloom (Sakshaug and Slagstad, 1991). It is feasible that stronger stratification in Ameralik at the location of the bloom initiation resulted in earlier bloom onset in 2019, although measurements capturing its onset are required to test this hypothesis. While Ameralik is more stratified than Nuup Kangerlua in July, the situation in May is less clear, with a similar fjord-wide stratification index for the upper 50 m layer but large station-by-station variation (Stuart-Lee et al., 2021). This situation may partially arise from the dispersed nature of snow melt and early runoff entering the fjord in May, compared to a better approximation of a point-source of discharge from the major river at the fjord head later in summer.

4.1.2. July

Local glacial meltwater input increases considerably between May and July (Kjeldsen et al., 2014; Mankoff et al., 2020). This is reflected in reduced salinity and increased stratification in the surface layers of both fjords in July (Figs. 2 and 3). During this period, production declined in Ameralik (Fig. 8a). The high SPM concentration in the surface waters of inner Ameralik (station AM10, Fig. 5a) coincided with low carbon content and low Chl *a* concentration, representing mostly inorganic glacially-derived material. Below the surface, Chl *a* concentration and carbon content increased, indicating that organic material constituted more of the SPM signal deeper in the water column (Figs. 5d and 8).

Meanwhile, conditions in Nuup Kangerlua are indicative of a summer bloom. Chl *a* concentration in Nuup Kangerlua increased to its peak

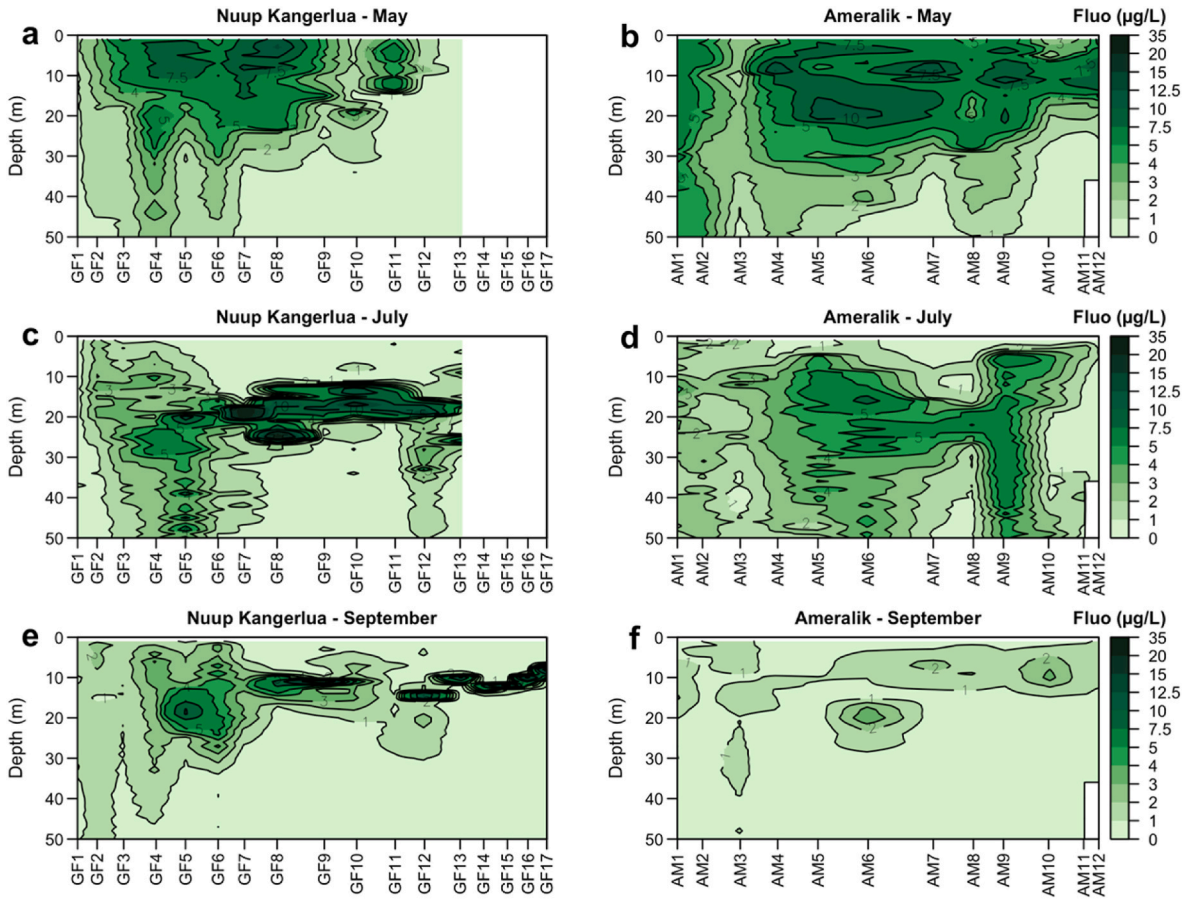

Fig. 7. Chlorophyll fluorescence concentrations in the upper 50 m of Nuup Kangerlua and Ameralik in (a, b) May, (c, d) July, and (e, f) September 2019. Station locations are indicated in Fig. 1.

of the studied months in July (Fig. 7), and nitrate and phosphate concentrations in the upper 20 m underwent a larger depletion than in Ameralik during this period (Fig. 6). Inner-fjord peaks in SPM (station GF13, Fig. 5a) had low carbon content and coincided with low Chl *a* concentration, while the mid-fjord peak at station GF7 was composed more of biological material, as seen from the high carbon content and Chl *a* concentration (Figs. 5d and 8a). In contrast to the spring bloom, summer blooms in Nuup Kangerlua are stimulated by upwelled nutrients related to subglacial discharge (Meire et al., 2017). Multi-year monitoring in this fjord has shown that peak production in the summer bloom can occasionally exceed that of the spring bloom (Juul-Pedersen et al., 2015), although a precise comparison of bloom magnitude in 2019 is challenging from monthly-resolution data.

4.1.3. September

By September, glacial meltwater input had declined (Kjeldsen et al., 2014; Mankoff et al., 2020), resulting in higher surface salinity and weakened haloclines across both fjords (Figs. 2 and 3). In combination with increased winds, these conditions led to increased surface mixing and more deep-water upwelling, in line with existing seasonal observations from these fjords (Mortensen et al., 2011, 2018; Stuart-Lee et al., 2021).

Upper water column concentrations of nutrients and Chl *a* were relatively low in both fjords, though we observe some remaining areas of high Chl *a* biomass in the inner fjord of Nuup Kangerlua. These occur from stations GF5 to GF17, peaking at a depth of ~10–20 m and are most concentrated in the inner fjord, suggesting the same 'upwelling' mechanism as in July (Fig. 7e). The elevated Chl *a* concentration indicates an extended bloom period in Nuup Kangerlua, likely composed of diatoms (Krawczyk et al., 2015, 2018), that was not matched in Ameralik. Diatoms are known to be the dominant species during the summer bloom in Nuup Kangerlua in connection with a favourable Si:N ratio that results from glacial runoff, and this dominance usually continues into autumn (Krawczyk et al., 2015, 2018; Meire et al., 2016). Although diatoms represent a large part of the phytoplankton biomass in these fjords, their size (typically larger than 20 µm) excludes them from the flow cytometry method used in this study, explaining the lack of correspondingly high cell counts. Our sampling timing in September appears to coincide with the decline of this bloom, in line with low remaining nutrient concentrations and the expected decline in runoff (Mankoff et al., 2020). The spatial distribution of Chl *a* suggests that the phytoplankton distribution may be following the deepening nitricline in the water column.

In Ameralik, cell counts increased across both pico- and nano-phytoplankton ranges while total Chl *a* was reduced (Fig. 8). A greater than 2-fold increase from July in picophytoplankton abundance across the fjord was largely due to the growth of the cyanobacterium *Synechococcus* (Fig. 8b). *Synechococcus* peaked at a depth of 5 m, reaching high abundances of 1.4×10^5 and 1.6×10^5 cells/ml (stations AM7 and AM10). Factors affecting *Synechococcus* distribution are not well understood, though they are known to be fast replicating, and tolerant to oligotrophic and low salinity environments (Partensky et al., 1999), which are conditions that describe the upper water column of Ameralik in September (Fig. 3e and f, 6). While not typically associated with Arctic picophytoplankton communities, *Synechococcus* has recently been observed at high abundances in the Fram Strait (79°N), with comparably large increases between summer and autumn (Paulsen et al., 2016; von Jackowski et al., 2022).

Both fjords showed indications of increased remineralisation through the sampled seasons, with mean ammonium concentrations

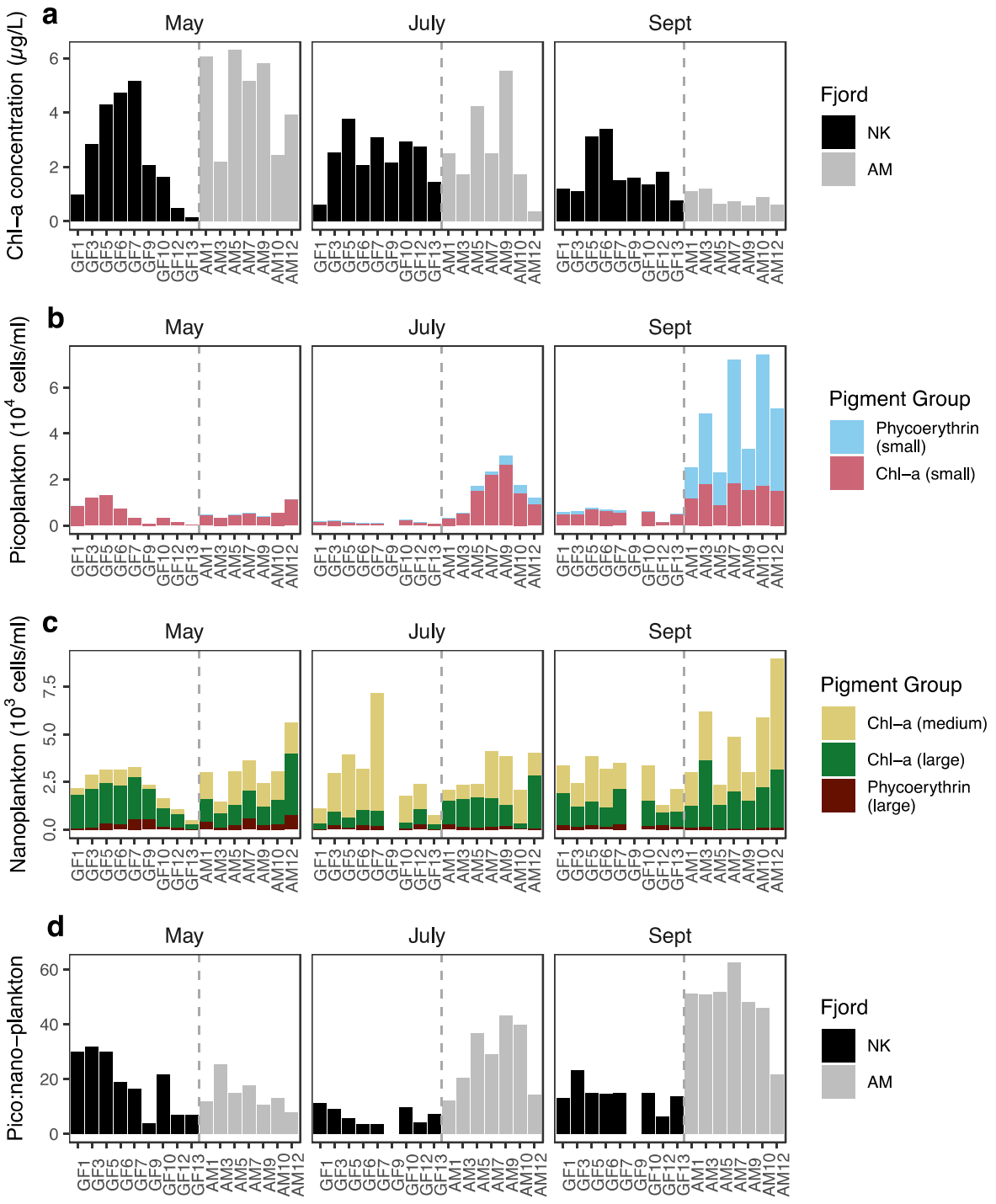

Fig. 8. Variation in mean values in the upper 40 m of the water column for (a) Chl *a* concentration, (b) picophytoplankton abundance, (c) nanophytoplankton abundance, and (d) ratio of pico-to nanophytoplankton abundance in Nuup Kangerlua and Ameralik in May, July and September 2019. Station locations are indicated in Fig. 1. At station GF9, pico- and nanophytoplankton counts are only available for May. Phycoerythrin is a proxy for the presence of *Synechococcus*.

(and the ratio of ammonium to nitrate) increasing similarly in both fjords. Higher ammonium concentrations occurred in Ameralik and a moderate negative Pearson correlation ($r = -0.5$, $p < 0.005$) was found between ammonium and Chl *a* concentration in July and September in Ameralik only, indicating more remineralisation than in Nuup Kangerlua. A further confounding factor in interpreting these trends is the potentially high rate of mortality within turbid particle plumes, particularly of filter feeding zooplankton. This phenomenon is described in Nuup Kangerlua (although at very high particle loads not observed in this study; Arendt et al., 2011) and several other turbid fjord systems around the Arctic (Węslawski et al., 1998; Hop et al., 2002; Arimitsu et al., 2012) and may exert 'top-down' effects on local ecosystem structure in addition to 'bottom-up' effects from shifts in resource (nutrient, organic carbon and light) availability (Larsen et al., 2015). Viral loads may also be reduced by high turbidity via adsorption of virions to glacial SPM, although the ecosystem and biogeochemical effects of this are yet to be extensively studied (Maat et al., 2019).

4.2. Summer bloom and fjord circulation

Circulation patterns are largely responsible for the transport of phytoplankton within a fjord and for the exchange of cells and nutrients with the coastal region. During the meltwater period, the estuarine circulation resulting from the inflow of surface meltwater runoff in the inner regions of fjords has been linked to a high import of marine organic matter, whereby the compensation current imports more organic matter than is exported in the fresher layer above (Sørensen et al., 2015). The same effect operates for macronutrients, whereby saline inflow at depth brings increased concentrations of all macronutrients into the fjord and surface outflow concentrations are more depleted (Meire et al., 2017). Below this estuarine circulation layer, a subglacial circulation arises in fjords with marine-terminating glaciers, driven by the subsurface release of glacial freshwater (Motyka et al., 2003; Rignot et al., 2010). This is associated with the advection of phytoplankton biomass from the inner to outer fjord during summer (Juul-Pedersen et al., 2015). The productive waters in-fjord of Nuup Kangerlua in summer 2019, identified by the high Chl *a* concentrations around stations GF8-GF12 and occurring at ~15 m depth, are likely connected to this subglacial discharge and associated nutrient supply, which results in new production.

Less is known about the connection between phytoplankton and intermediate baroclinic circulation, which is present year-round in Nuup Kangerlua and Ameralik (Mortensen et al., 2011, 2014; Stuart-Lee et al., 2021). This circulation is the characteristic mode in summer when the combination of tidal mixing in the outer sill region and warming and freshening of surface fjord water results in the outer fjord water becoming less dense than the inner fjord. This drives an in-fjord current in the upper water column, and a compensation out-flow below, lowering the isopycnals in the fjord (Mortensen et al., 2011, 2014).

We propose a link between this circulation and the spatial patterns of phytoplankton in Ameralik and Nuup Kangerlua in summer 2019 (Fig. 9). In July, a well-mixed region can be observed at the mouth of Nuup Kangerlua (stations GF1-3, Fig. 2c and d, 7c). In the region around stations GF5-GF8, there is an interaction of water masses where the outflow layer of the subglacial circulation, identified by its lower temperature compared to outer fjord water (Fig. 2c), meets this returning inflow from the intermediate baroclinic circulation (Mortensen et al., 2011). At these stations, patches of high Chl *a* concentration occurred at ~20 m depth (Fig. 7c). We propose that these productive waters relate not only to the subglacial water, but also to the warmer re-circulating inflow of the intermediate baroclinic circulation (e.g., Mortensen et al., 2014). This inflow increases the availability of nutrients higher in the water column (than would otherwise be the case) and contains advected phytoplankton cells.

We see a similarly well-mixed region at the mouth of Ameralik in July (stations AM1-2, Fig. 3c and d, 7d). The bloom appears from station

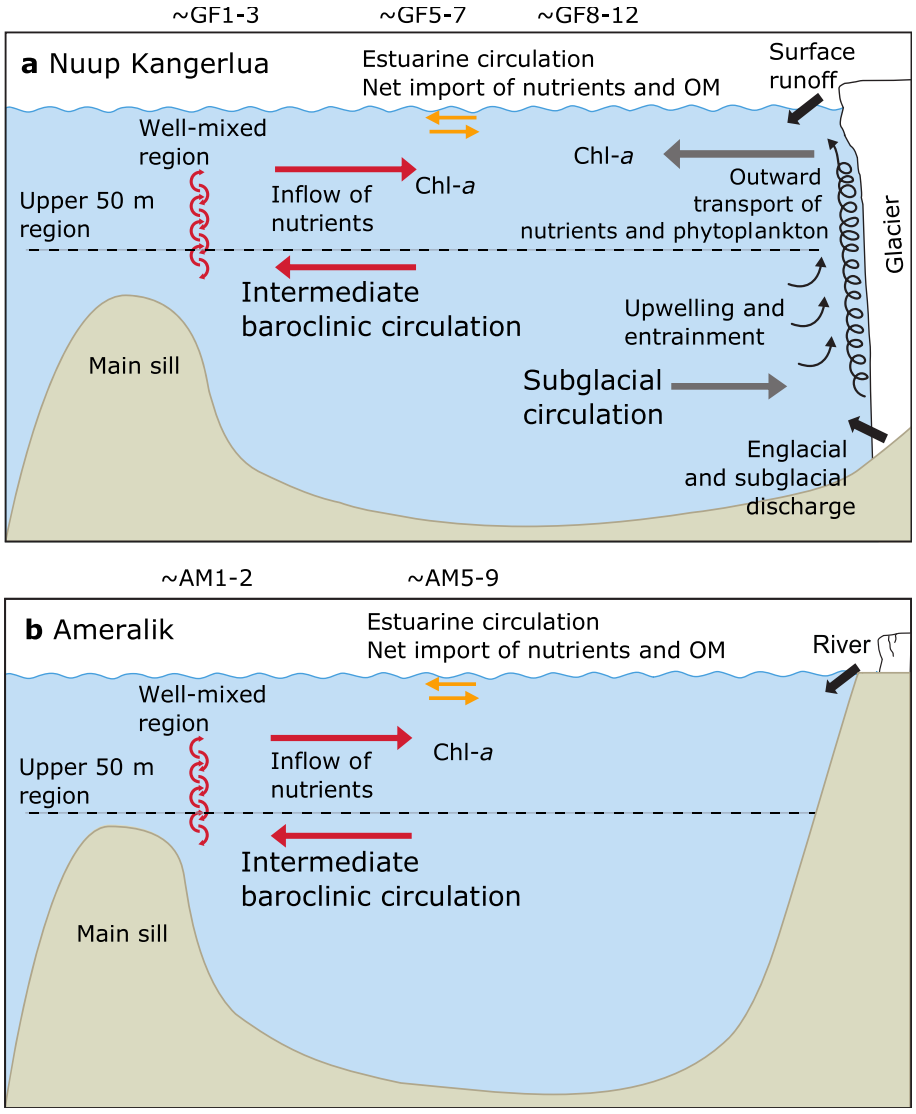

Fig. 9. Fjord schematic of connections between circulation patterns and phytoplankton distribution in summer in (a) Nuup Kangerlua and (b) Ameralik. The diagram is not to scale, and the upper 50 m has been exaggerated for clarity. Net effects of estuarine circulation are represented by yellow arrows, intermediate baroclinic circulation by red arrows, and subglacial circulation by grey arrows. This circulation model of Nuup Kangerlua is as per Mortensen et al. (2011). (For interpretation of the references to color in this figure legend, the reader is referred to the Web version of this article.)

AM5 at ~15 m depth, deepening around stations AM6-9 and is absent by station AM10 in the inner fjord. As for the outer fjord waters of Nuup Kangerlua, this distribution in Ameralik may be related to the sill-region mixing and intermediate baroclinic circulation, whereby the water recirculated back into the fjord at a shallower depth allows a bloom to develop via increased nutrient availability. In contrast, the subglacial circulation pattern (and associated out-fjord advection of phytoplankton cells) is not applicable to Ameralik due to the lack of a marine-terminating glacier.

4.3. Pico- and nanophytoplankton

Pico- and nanophytoplankton abundances and their relative proportions are comparable across Nuup Kangerlua and Ameralik in May. This is consistent with the shared drivers of spring blooms and the expectation that, following over-winter inflow, both fjords have similar nutrient availabilities and phytoplankton compositions prior to the bloom onset. However, large differences develop as the seasons progress. While picophytoplankton abundance declines in Nuup Kangerlua between May and July, both the abundance and proportion of picophytoplankton becomes considerably higher in Ameralik (Fig. 8b,d). By September, the mean ratio of pico-to nanophytoplankton in the upper 40 m layer is almost 4 times higher in Ameralik than in Nuup Kangerlua, illustrating the increasing representation of picophytoplankton in Ameralik (Fig. 8d).

Smaller average body sizes have been observed in a wide range of aquatic communities as an ecological response to climate change, with increasing temperatures proposed as one of the major drivers (Daufresne et al., 2009; Morán et al., 2010; Sheridan and Bickford, 2011). In mesocosm experiments looking specifically at temperature effects on phytoplankton, Sommer and Lengfellner (2008) linked higher temperatures to smaller cells, lower peak phytoplankton biomass, fewer diatoms, and higher relative biomass of picophytoplankton. While this experiment was setup to reflect temperate waters and not high latitude conditions, we see a similar picture within the small phytoplankton community (i.e., pico- and nanophytoplankton) in Ameralik and Nuup Kangerlua in July and September. The upper 50 m layer of Ameralik becomes warmer than that of Nuup Kangerlua from July and the mean difference between the fjords rises to 2 °C in September (Fig. 2c,e, 3c,e). In Ameralik a moderate correlation between temperature and the ratio of pico-to nanophytoplankton (0.6, $p < 0.005$) is found in July and September, which is mirrored less strongly in Nuup Kangerlua (0.5 and 0.4, $p < 0.005$), indicating that the temperature differences may be related to the size composition in these fjords.

Small-celled picophytoplankton (0.2–2 μm) are also known to be more dominant in oligotrophic conditions, where their larger surface-area-to-volume ratio is advantageous for nutrient acquisition (Raven, 1998; Agawin et al., 2000). This advantage has been observed in the Arctic, where picophytoplankton thrive in the stratified and low nutrient conditions of the waters undergoing freshening (Li et al., 2009). In a study looking at the size range of phytoplankton in Young Sound in Northeast Greenland, Middelbo et al. (2017) found a dominance of small cells (<10 μm, i.e., comprising both pico- and nanophytoplankton) in the inner fjord, close to the source of runoff where the surface water was turbid and brackish, and larger cells (>10 μm) dominating further towards the fjord mouth. While disentangling the multiple factors linked to cell size is scientifically challenging, we observe a similar steady gradient within a smaller cell size range in Ameralik in July. Picophytoplankton dominate towards the inner fjord where the waters were stratified and turbid due to the freshwater runoff. This contrasts with Nuup Kangerlua, which maintained a gradient of increasing picophytoplankton proportion in the opposite direction (out-fjord) from May to July.

A shift towards smaller cells and, in turn, smaller predators has been predicted on a wider scale across the Arctic (Li et al., 2009; Onda et al., 2017). In Young Sound, Middelbo et al. (2017) found that the dominance of small phytoplankton cells (<10 μm) was coincident with a decline in zooplankton grazing and secondary production. As our study is limited to pico- and nanophytoplankton, we cannot generalise across the phytoplankton community as a whole. Within the scope of small phytoplankton, however, this fjord comparison is in line with prior findings from Young Sound, suggesting that an increasing representation of picophytoplankton will be one response to the retreating of marine-terminating glaciers onto land, through increased stratification and turbidity, warmer surface water and lower nutrient availability in the photic zone.

5. Conclusions

Two fjords in the same climatic region of west Greenland displayed similar spring bloom dynamics at the onset of the meltwater season in 2019 but diverged in productivity and pico- and nanophytoplankton abundances over summer. Nuup Kangerlua was distinguished by a sustained second summer bloom and higher overall Chl *a* fluorescence than Ameralik in summer and autumn. Pico- (<2 μm) and nanophytoplankton (2–20 μm) abundances were comparable between fjords in May, but differences grew with the seasons. By September, much higher abundances of pico- (<2 μm) and nanophytoplankton (2–20 μm) were observed in Ameralik, alongside high cyanobacteria growth. The greater representation of picophytoplankton among small phytoplankton identified in Ameralik is likely related to a combination of higher surface water temperatures, stronger stratification (reduced nutrient availability) and reduced light availability. These findings support the hypothesis that smaller cells may be better adapted to cope with the environmental stressors associated with the retreat of marine-terminating glaciers and may therefore represent a greater proportion of fjord phytoplankton communities in the future. Lower overall summer productivity in Ameralik is partially attributed to the absence of subglacial discharge from marine-terminating glaciers, though we suggest that the summer bloom in Nuup Kangerlua is not solely driven by the subglacial circulation, but that the inflow at subsurface depths due to the intermediate baroclinic circulation also plays a role in increasing nutrient availability at shallower depths. This highlights the complex links between circulation patterns and bloom dynamics in fjords.

CRediT authorship contribution statement

A.E. Stuart-Lee: Writing – review & editing, Writing – original draft, Investigation, Formal analysis, Data curation, Conceptualization. **J. Mortensen:** Writing – review & editing. **T. Juul-Pedersen:** Writing – review & editing. **J.J. Middelburg:** Writing – review & editing. **K. Soetaert:** Writing – review & editing. **M.J. Hopwood:** Writing – review & editing. **A. Engel:** Writing – review & editing, Data curation. **L. Meire:** Writing – review & editing, Supervision, Data curation, Conceptualization.

Declaration of competing interest

The authors declare that they have no known competing financial interests or personal relationships that could have appeared to influence the work reported in this paper.

Data availability

Data will be made available on request.

Acknowledgements

This study received financial support from the Greenland Climate Research Centre. The study was conducted in collaboration with the MarineBasis Nuuk monitoring program, part of Greenland Ecosystem Monitoring (GEM), and forms a contribution to the Arctic Science

Partnership (ASP). Data from the Greenland Ecosystem Monitoring Programme (www.g-e-m.dk) were provided by the Greenland Institute of Natural Resources, Nuuk, Greenland. Laboratory analysis was supported by DFG award number HO 6321/1-1 to Mark Hopwood at GEOMAR. L. Meire was funded by research program VENI with project 016.Veni.192.150 from the Dutch Research Council (NWO). J. Middelburg was supported by the Netherlands Earth System Science Centre. We thank Tania Klüver at GEOMAR for running the flow cytometry samples. We would also like to thank Flemming Heinrich, Else Ostermann, and the crew of RV SANNA, Peter Rosvig Pedersen of the Polar Diver, Anders Pedersen, and the crew of the Tulu for their field assistance.

Appendix A. Supplementary data

Supplementary data to this article can be found online at https://doi.org/10.1016/j.ecss.2023.108271.

References

Agawin, N.S.R., Duarte, C.M., Agustí, S., 2000. Nutrient and temperature control of the contribution of picoplankton to phytoplankton biomass and production. Limnol. Oceanogr. 45 (3), 591–600. https://doi.org/10.4319/lo.2000.45.3.0591.

Arendt, K.E., Dutz, J., Jonasdottir, S.H., Jung-Madsen, S., Mortensen, J., Moller, E.F., Nielsen, T.G., 2011. Effects of suspended sediments on copepods feeding in a glacial influenced sub-Arctic fjord. J. Plankton Res. 33 (10), 1526–1537. https://doi.org/10.1093/plankt/fbr054.

Arendt, K.E., Nielsen, T.G., Rysgaard, S., Tönnesson, K., 2010. Differences in plankton community structure along the Godthåbsfjord, from the Greenland Ice Sheet to offshore waters. Mar. Ecol. Prog. Ser. 401, 49–62. https://doi.org/10.3354/meps08368.

Arimitsu, M.L., Piatt, J.F., Madison, E.N., Conaway, J.S., Hillgruber, N., 2012. Oceanographic gradients and seabird prey community dynamics in glacial fjords: glacial fjord marine habitat. Fish. Oceanogr. 21 (2–3), 148–169. https://doi.org/10.1111/j.1365-2419.2012.00616.x.

Bhatia, M.P., Waterman, S., Burgess, D.O., Williams, P.L., Bundy, R.M., Mellett, T., Roberts, M., Bertrand, E.M., 2021. Glaciers and nutrients in the Canadian Arctic Archipelago marine system. Global Biogeochem. Cycles 35 (8). https://doi.org/10.1029/2021GB006976.

Bridier, G., Olivier, F., Chauvaud, L., Sejr, M.K., Grall, J., 2021. Food source diversity, trophic plasticity, and omnivory enhance the stability of a shallow benthic food web from a high-Arctic fjord exposed to freshwater inputs. Limnol. Oceanogr. 66 (S1) https://doi.org/10.1002/lno.11688.

Calleja, M. Ll, Kerhervé, P., Bourgeois, S., Kędra, M., Leynaert, A., Devred, E., Babin, M., Morata, N., 2017. Effects of increase glacier discharge on phytoplankton bloom dynamics and pelagic geochemistry in a high Arctic fjord. Prog. Oceanogr. 159, 195–210. https://doi.org/10.1016/j.pocean.2017.07.005.

Cape, M.R., Straneo, F., Beaird, N., Bundy, R.M., Charette, M.A., 2019. Nutrient release to oceans from buoyancy-driven upwelling at Greenland tidewater glaciers. Nat. Geosci. 12 (1), 34–39. https://doi.org/10.1038/s41561-018-0268-4.

Daufresne, M., Lengfellner, K., Sommer, U., 2009. Global warming benefits the small in aquatic ecosystems. Proc. Natl. Acad. Sci. USA 106 (31), 12788–12793. https://doi.org/10.1073/pnas.0902080106.

Dunse, T., Dong, K., Aas, K.S., Stige, L.C., 2022. Regional-scale phytoplankton dynamics and their association with glacier meltwater runoff in Svalbard. Biogeosciences 19 (2), 271–294. https://doi.org/10.5194/bg-19-271-2022.

Grasshoff, K., Kremling, K., Ehrhardt, M. (Eds.), 1999. Methods of Seawater Analysis. John Wiley & Sons.

Grosse, J., van Breugel, P., Boschker, H.T.S., 2015. Tracing carbon fixation in phytoplankton-compound specific and total 13C incorporation rates. Limnol Oceanogr. Methods 13 (6), 288–302. https://doi.org/10.1002/lom3.10025.

Halbach, L., Vihtakari, M., Duarte, P., Everett, A., Granskog, M.A., Hop, H., Kauko, H.M., Kristiansen, S., Myhre, P.I., Pavlov, A.K., Pramanik, A., Tatarek, A., Torsvik, T., Wiktor, J.M., Wold, A., Wulff, A., Steen, H., Assmy, P., 2019. Tidewater glaciers and bedrock characteristics control the phytoplankton growth environment in a fjord in the Arctic. Front. Mar. Sci. 6, 254. https://doi.org/10.3389/fmars.2019.00254.

Holding, J.M., Markager, S., Juul-Pedersen, T., Paulsen, M.L., Møller, E.F., Meire, L., Sejr, M.K., 2019. Seasonal and spatial patterns of primary production in a high-latitude fjord affected by Greenland Ice Sheet run-off. Biogeosciences 16 (19), 3777–3792. https://doi.org/10.5194/bg-16-3777-2019.

Hop, H., Pearson, T., Hegseth, E.N., Kovacs, K.M., Wiencke, C., Kwasniewski, S., Eiane, K., Mehlum, F., Gulliksen, B., Wlodarska-Kowalczuk, M., Lydersen, C., Weslawski, J.M., Cochrane, S., Gabrielsen, G.W., Leakey, R.J.G., Lønne, O.J., Zajaczkowski, M., Falk-Petersen, S., Kendall, M., et al., 2002. The marine ecosystem of Kongsfjorden, Svalbard. Polar Res. 21 (1), 167–208. https://doi.org/10.3402/polar.v21i1.6480.

Howat, I.M., Eddy, A., 2011. Multi-decadal retreat of Greenland's marine-terminating glaciers. J. Glaciol. 57 (203), 389–396. https://doi.org/10.3189/002214311796905631.

Juul-Pedersen, T., Arendt, K., Mortensen, J., Blicher, M., Søgaard, D., Rysgaard, S., 2015. Seasonal and interannual phytoplankton production in a sub-Arctic tidewater outlet glacier fjord, SW Greenland. Mar. Ecol. Prog. Ser. 524, 27–38. https://doi.org/10.3354/meps11174.

Kanna, N., Sugiyama, S., Ohashi, Y., Sakakibara, D., Fukamachi, Y., Nomura, D., 2018. Upwelling of macronutrients and dissolved inorganic carbon by a subglacial freshwater driven plume in Bowdoin fjord, Northwestern Greenland. J. Geophys. Res.: Biogeosciences 123 (5), 1666–1682. https://doi.org/10.1029/2017JG004248.

King, M.D., Howat, I.M., Candela, S.G., Noh, M.J., Jeong, S., Noël, B.P., et al., 2020. Dynamic ice loss from the Greenland Ice Sheet driven by sustained glacier retreat. Communications Earth & Environment 1 (1), 1–7.

Kjeldsen, K.K., Mortensen, J., Bendtsen, J., Petersen, D., Lennert, K., Rysgaard, S., 2014. Ice-dammed lake drainage cools and raises surface salinities in a tidewater outlet glacier fjord, west Greenland. J. Geophys. Res.: Earth Surf. 119 (6), 1310–1321. https://doi.org/10.1002/2013JF003034.

Krawczyk, D.W., Witkowski, A., Juul-Pedersen, T., Arendt, K.E., Mortensen, J., Rysgaard, S., 2015. Microplankton succession in a SW Greenland tidewater glacial fjord influenced by coastal inflows and run-off from the Greenland Ice Sheet. Polar Biol. 38 (9), 1515–1533. https://doi.org/10.1007/s00300-015-1715-y.

Krawczyk, D.W., Meire, L., Lopes, C., Juul-Pedersen, T., Mortensen, J., Li, C.L., Krogh, T., 2018. Seasonal succession, distribution, and diversity of planktonic protists in relation to hydrography of the Godthåbsfjord system (SW Greenland). Polar Biol. 41 (10), 2033–2052. https://doi.org/10.1007/s00300-018-2343-0.

Langen, P.L., Mottram, R.H., Christensen, J.H., Boberg, F., Rodehacke, C.B., Stendel, M., van As, D., Ahlstrøm, A.P., Mortensen, J., Rysgaard, S., Petersen, D., Svendsen, K.H., Aðalgeirsdóttir, G., Cappelen, J., 2015. Quantifying energy and mass fluxes controlling Godthåbsfjord freshwater input in a 5-km simulation (1991–2012). J. Clim. 28 (9), 3694–3713. https://doi.org/10.1175/JCLI-D-14-00271.1.

Larsen, A., Egge, J.K., Nejstgaard, J.C., Di Capua, I., Thyrhaug, R., Bratbak, G., Thingstad, T.F., 2015. Contrasting response to nutrient manipulation in Arctic mesocosms are reproduced by a minimum microbial food web model. Limnol. Oceanogr. 60 (2), 360–374. https://doi.org/10.1002/lno.10025.

Li, W.K.W., McLaughlin, F.A., Lovejoy, C., Carmack, E.C., 2009. Smallest Algae thrive as the Arctic ocean freshens. Science 326 (5952). https://doi.org/10.1126/science.1179798, 539–539.

Lyngsgaard, M.M., Markager, S., Richardson, K., 2014. Changes in the vertical distribution of primary production in response to land-based nitrogen loading. Limnol. Oceanogr. 59 (5), 1679–1690. https://doi.org/10.4319/lo.2014.59.5.1679.

Maat, D., Prins, M., Brussaard, C., 2019. Sediments from Arctic tide-water glaciers remove coastal marine viruses and delay host infection. Viruses 11 (2), 123. https://doi.org/10.3390/v11020123.

Mankoff, K.D., Noël, B., Fettweis, X., Ahlstrøm, A.P., Colgan, W., Kondo, K., Langley, K., Sugiyama, S., van As, D., Fausto, R.S., 2020. Greenland liquid water discharge from 1958 through 2019. Earth Syst. Sci. Data 12 (4), 2811–2841. https://doi.org/10.5194/essd-12-2811-2020.

Meire, L., Meire, P., Struyf, E., Krawczyk, D.W., Arendt, K.E., Yde, J.C., Juul Pedersen, T., Hopwood, M.J., Rysgaard, S., Meysman, F.J.R., 2016. High export of dissolved silica from the Greenland ice sheet: silica export the ice sheet. Geophys. Res. Lett. 43 (17), 9173–9182. https://doi.org/10.1002/2016GL070191.

Meire, L., Mortensen, J., Meire, P., Juul-Pedersen, T., Sejr, M.K., Rysgaard, S., Nygaard, R., Huybrechts, P., Meysman, F.J.R., 2017. Marine-terminating glaciers sustain high productivity in Greenland fjords. Global Change Biol. 23 (12), 5344–5357. https://doi.org/10.1111/gcb.13801.

Mernild, S.H., Liston, G.E., 2012. Greenland freshwater runoff. Part II: distribution and trends, 1960–2010. J. Clim. 25 (17), 6015–6035. https://doi.org/10.1175/JCLI-D-11-00592.1.

Middelbo, A.B., Sejr, M.K., Arendt, K.E., Møller, E.F., 2017. Impact of glacial meltwater on spatiotemporal distribution of copepods and their grazing impact in Young Sound NE, Greenland: impact of meltwater on copepod carbon cycling. Limnol. Oceanogr. 63 (1), 322–336. https://doi.org/10.1002/lno.10633.

Morán, X.A.G., López-Urrutia, Á., Calvo-Díaz, A., Li, W.K.W., 2010. Increasing importance of small phytoplankton in a warmer ocean. Global Change Biol. 16 (3), 1137–1144. https://doi.org/10.1111/j.1365-2486.2009.01960.x.

Mortensen, J., Bendtsen, J., Lennert, K., Rysgaard, S., 2014. Seasonal variability of the circulation system in a west Greenland tidewater outlet glacier fjord, Godthåbsfjord (64°N): Godthåbsfjord. J. Geophys. Res.: Earth Surf. 119 (12), 2591–2603. https://doi.org/10.1002/2014JF003267.

Mortensen, J., Bendtsen, J., Motyka, R.J., Lennert, K., Truffer, M., Fahnestock, M., Rysgaard, S., 2013. On the seasonal freshwater stratification in the proximity of fast-flowing tidewater outlet glaciers in a sub-Arctic sill fjord: Godthåbsfjord. J. Geophys. Res.: Oceans 118 (3), 1382–1395. https://doi.org/10.1002/jgrc.20134.

Mortensen, J., Lennert, K., Bendtsen, J., Rysgaard, S., 2011. Heat sources for glacial melt in a sub-Arctic fjord (Godthåbsfjord) in contact with the Greenland Ice Sheet. J. Geophys. Res.: Oceans 116 (C1). https://doi.org/10.1029/2010JC006528.

Mortensen, J., Rysgaard, S., Arendt, K.E., Juul-Pedersen, T., Søgaard, D.H., Bendtsen, J., Meire, L., 2018. Local coastal water masses control heat levels in a west Greenland tidewater outlet glacier fjord. J. Geophys. Res.: Oceans 123 (11), 8068–8083. https://doi.org/10.1029/2018JC014549.

Mortensen, J., Rysgaard, S., Winding, M.H.S., Juul-Pedersen, T., Arendt, K.E., Lund, H., Stuart-Lee, A.E., Meire, L., 2022. Multidecadal water mass dynamics on the west Greenland shelf. J. Geophys. Res.: Oceans 127 (7), e2022JC018724.

Motyka, R.J., Hunter, L., Echelmeyer, K.A., Connor, C., 2003. Submarine melting at the terminus of a temperate tidewater glacier, LeConte Glacier, Alaska, U.S.A. Ann. Glaciol. 36, 57–65. https://doi.org/10.3189/172756403781816374.

Mouginot, J., Rignot, E., Bjørk, A.A., van den Broeke, M., Millan, R., Morlighem, M., Noël, B., Scheuchl, B., Wood, M., 2019. Forty-six years of Greenland Ice Sheet mass balance from 1972 to 2018. Proc. Natl. Acad. Sci. USA 116 (19), 9239–9244. https://doi.org/10.1073/pnas.1904242116.

Murray, C., Markager, S., Stedmon, C.A., Juul-Pedersen, T., Sejr, M.K., Bruhn, A., 2015. The influence of glacial melt water on bio-optical properties in two contrasting Greenlandic fjords. Estuar. Coast Shelf Sci. 163, 72–83. https://doi.org/10.1016/j.ecss.2015.05.041.

Onda, D.F.L., Medrinal, E., Comeau, A.M., Thaler, M., Babin, M., Lovejoy, C., 2017. Seasonal and Interannual Changes in Ciliate and Dinoflagellate Species Assemblages in the Arctic Ocean (Amundsen Gulf, Beaufort Sea, Canada). Front. Mar. Sci. 4 https://doi.org/10.3389/fmars.2017.00016.

Partensky, F., Blanchot, Jean, Vaulot, D., 1999. Differential distribution and ecology of Prochlorococcus and Synechococcus in oceanic waters: A review. Bulletin de l'institut Océanographique de Monaco, spécial 19, 457–475.

Paulsen, M.L., Dore, H., Garczarek, L., Seuthe, L., Mueller, O., Sandaa, R.A., Bratbak, G., Larsen, A., 2016. Synechococcus in the Atlantic gateway to the Arctic Ocean. Front. Mar. Sci. 3, 191.

Piwosz, K., Walkusz, W., Hapter, R., Wieczorek, P., Hop, H., Wiktor, J., 2009. Comparison of productivity and phytoplankton in a warm (Kongsfjorden) and a cold (Hornsund) Spitsbergen fjord in mid-summer 2002. Polar Biol. 32 (4), 549–559. https://doi.org/10.1007/s00300-008-0549-2.

R Core Team, 2013. R: A Language and Environment for Statistical Computing. R Development Core Team, Vienna, Austria.

Randelhoff, A., Holding, J., Janout, M., Sejr, M.K., Babin, M., Tremblay, J.-É., Alkire, M. B., 2020. Pan-Arctic Ocean Primary Production Constrained by Turbulent Nitrate Fluxes. Front. Mar. Sci. 7, 150. https://doi.org/10.3389/fmars.2020.00150.

Raven, J.A., 1998. The twelfth Tansley Lecture. Small is beautiful: The picophytoplankton. Funct. Ecol. 12 (4), 503–513. https://doi.org/10.1046/j.1365-2435.1998.00233.x.

Richter, A., Rysgaard, S., Dietrich, R., Mortensen, J., Petersen, D., 2011. Coastal tides in West Greenland derived from tide gauge records. Ocean Dynam. 61 (1), 39–49. https://doi.org/10.1007/s10236-010-0341-z.

Rignot, E., Koppes, M., Velicogna, I., 2010. Rapid submarine melting of the calving faces of West Greenland glaciers. Nat. Geosci. 3 (3), 187–191. https://doi.org/10.1038/ngeo765.

Rysgaard, S., Boone, W., Carlson, D., Sejr, M.K., Bendtsen, J., Juul-Pedersen, T., Lund, H., Meire, L., Mortensen, J., 2020. An Updated View on Water Masses on the pan-West Greenland Continental Shelf and Their Link to Proglacial Fjords. J. Geophys. Res.: Oceans 125 (2). https://doi.org/10.1029/2019JC015564.

Rysgaard, S., Vang, T., Stjernholm, M., Rasmussen, B., Windelin, A., Kiilsholm, S., 2003. Physical Conditions, Carbon Transport, and Climate Change Impacts in a Northeast Greenland Fjord. Arctic Antarct. Alpine Res. 35 (3), 301–312. https://doi.org/10.1657/1523-0430(2003)035[0301:PCCTAC]2.0.CO;2.

Sakshaug, E., Slagstad, D., 1991. Light and productivity of phytoplankton in polar marine ecosystems: A physiological view. Polar Res. 10 (1), 69–86. https://doi.org/10.3402/polar.v10i1.6729.

Sheridan, J.A., Bickford, D., 2011. Shrinking body size as an ecological response to climate change. Nat. Clim. Change 1 (8), 401–406. https://doi.org/10.1038/nclimate1259.

Sommer, U., Lengfellner, K., 2008. Climate change and the timing, magnitude, and composition of the phytoplankton spring bloom. Global Change Biol. 14 (6), 1199–1208. https://doi.org/10.1111/j.1365-2486.2008.01571.x.

Sørensen, H., Meire, L., Juul-Pedersen, T., de Stigter, H., Meysman, F., Rysgaard, S., Thamdrup, B., Glud, R., 2015. Seasonal carbon cycling in a Greenlandic fjord: An integrated pelagic and benthic study. Mar. Ecol. Prog. Ser. 539, 1–17. https://doi.org/10.3354/meps11503.

Straneo, F., Sutherland, D.A., Stearns, L., Catania, G., Heimbach, P., Moon, T., Cape, M. R., Laidre, K.L., Barber, D., Rysgaard, S., Mottram, R., Olsen, S., Hopwood, M.J., Meire, L., 2019. The Case for a Sustained Greenland Ice Sheet-Ocean Observing System (GrIOOS). Front. Mar. Sci. 6, 138. https://doi.org/10.3389/fmars.2019.00138.

Stuart-Lee, A.E., Mortensen, J., van der Kaaden, A.-S., Meire, L., 2021. Seasonal Hydrography of Ameralik: A Southwest Greenland Fjord Impacted by a Land-Terminating Glacier. J. Geophys. Res.: Oceans 126 (12). https://doi.org/10.1029/2021JC017552.

Szeligowska, M., Trudnowska, E., Boehnke, R., Dąbrowska, A.M., Dragańska-Deja, K., Deja, K., Darecki, M., Błachowiak-Samołyk, K., 2021. The interplay between plankton and particles in the Isfjorden waters influenced by marine- and land-terminating glaciers. Sci. Total Environ. 780, 146491 https://doi.org/10.1016/j.scitotenv.2021.146491.

Tremblay, J.-É., Michel, C., Hobson, K.A., Gosselin, M., Price, N.M., 2006. Bloom dynamics in early opening waters of the Arctic Ocean. Limnol. Oceanogr. 51 (2), 900–912. https://doi.org/10.4319/lo.2006.51.2.0900.

Tremblay, J.-É., Simpson, K., Martin, J., Miller, L., Gratton, Y., Barber, D., Price, N.M., 2008. Vertical stability and the annual dynamics of nutrients and chlorophyll fluorescence in the coastal, southeast Beaufort Sea. J. Geophys. Res.: Oceans 113 (C7), C07S90. https://doi.org/10.1029/2007JC004547.

Trudnowska, E., Dąbrowska, A.M., Boehnke, R., Zajączkowski, M., Blachowiak-Samolyk, K., 2020. Particles, protists, and zooplankton in glacier-influenced coastal Svalbard waters. Estuar. Coast Shelf Sci. 242, 106842 https://doi.org/10.1016/j.ecss.2020.106842.

Trusel, L.D., Das, S.B., Osman, M.B., Evans, M.J., Smith, B.E., Fettweis, X., McConnell, J. R., Noël, B.P.Y., van den Broeke, M.R., 2018. Nonlinear rise in Greenland runoff in response to post-industrial Arctic warming. Nature 564 (7734), 104–108. https://doi.org/10.1038/s41586-018-0752-4.

von Jackowski, A., Becker, K.W., Wietz, M., Bienhold, C., Zäncker, B., Nöthig, E.M., Engel, A., 2022. Variations of microbial communities and substrate regimes in the eastern Fram Strait between summer and fall. Environ. Microbiol. 24 (9), 4124–4236.

Węslawski, J.M., Legezyriska, J., 1998. Glaciers caused zooplankton mortality? J. Plankton Res. 20 (7), 1233–1240.